NATIONAL ADVISORY COMMITTEE FOR AERONAUTICS

TECHNICAL NOTE

No. 1723

A THEORETICAL INVESTIGATION OF THE EFFECT OF YAWING MOMENT DUE TO ROLLING ON LATERAL OSCILLATORY STABILITY

By Joseph L. Johnson and Leonard Sternfield

Langley Aeronautical Laboratory
Langley Field, Va.

Washington
October 1948

NATIONAL ADVISORY COMMITTEE FOR AERONAUTICS

TECHNICAL NOTE NO. 1723

A THEORETICAL INVESTIGATION OF THE EFFECT OF YAWING MOMENT DUE TO ROLLING ON LATERAL OSCILLATORY STABILITY

By Joseph L. Johnson and Leonard Sternfield

SUMMARY

The effect on lateral oscillatory stability of varying the value of the stability derivative C_{n_p} (yawing-moment coefficient due to rolling-angular-velocity factor) over a wide range of negative and positive values has been determined theoretically for a sweptback fighter airplane with loading conditions simulating an airplane with wing-tip fuel tanks and without wing-tip fuel tanks. Increasing C_{n_p} in a positive direction was shown to increase the damping of the short-period oscillation. For any given value of C_{n_p} the addition of the wing-tip tanks, which involved shifting fuel from the fuselage to the wing tip, decreased the damping of the short-period oscillation.

INTRODUCTION

Recent theoretical and experimental investigations (reference 1) have indicated that the stability derivative C_{n_p} (yawing-moment coefficient due to rolling-angular-velocity factor) may be greatly affected by sweep, aspect ratio, taper ratio, and lift coefficient. In fact, the value of C_{n_p}, which is normally negative in sign and proportional to lift coefficient for straight wings, has been found to vary from −0.10 to 0.30 over the lift range for highly swept wings. Calculations of reference 2 showed that even small variations in the value of C_{n_p} (−0.02 to 0.02) might have an appreciable effect on the neutral-oscillatory-stability boundary. In order to determine the effect on the oscillatory stability of extending the range of the variation of C_{n_p}, stability calculations were made in which C_{n_p} was varied systematically over a wide range of positive and negative values (−0.10 to 0.40).

The calculations were made for a sweptback, jet-propelled fighter-type airplane for two loading conditions. The loading conditions assumed were for the airplane with wing-tip fuel tanks and without wing-tip tanks. For the condition without wing-tip tanks an approximately equal quantity of fuel was assumed to be carried near the center of gravity.

SYMBOLS AND COEFFICIENTS

S	wing area, square feet
$\bar{c}$	mean aerodynamic chord, feet
V	airspeed, feet per second
b	wing span, feet
q	dynamic pressure, pounds per square foot
ρ	air density, slugs per cubic foot
W	weight, pounds
g	acceleration of gravity, feet per second per second
m	mass, slugs (W/g)
μ_b	relative density factor based on wing span $(m/\rho Sb)$
α	angle of attack of reference axis (fig. 1), degrees
η	angle of attack of principal longitudinal axis of airplane, positive when principal axis is above flight path at the nose (fig. 1), degrees
ϵ	angle between reference axis and principal axis, positive when reference axis is above principal axis at the nose (fig. 1), degrees
θ	angle between reference axis and horizontal axis, positive when reference axis is above horizontal axis at the nose (fig. 1), degrees
γ	angle of flight to horizontal axis, positive in a climb (fig. 1), degrees
ψ	angle of yaw, degrees or radians
β	angle of sideslip, degrees or radians
ϕ	angle of bank, radians
R	Routh's discriminant $(R = BCD - AD^2 - B^2E$ where A, B, C, D, and E are constants representing coefficients of the lateral stability equation)
k_{X_o}	radius of gyration about principal longitudinal axis, feet

k_{Z_o} radius of gyration about principal vertical axis, feet

K_{X_o} nondimensional radius of gyration about principal longitudinal axis $\left(k_{X_o}/b\right)$

K_{Z_o} nondimensional radius of gyration about principal vertical axis $\left(k_{Z_o}/b\right)$

K_X nondimensional radius of gyration about longitudinal stability axis $\left(\sqrt{K_{X_o}{}^2\cos^2\eta + K_{Z_o}{}^2\sin^2\eta}\right)$

K_Z nondimensional radius of gyration about vertical stability axis $\left(\sqrt{K_{Z_o}{}^2\cos^2\eta + K_{X_o}{}^2\sin^2\eta}\right)$

K_{XZ} nondimensional product-of-inertia parameter $\left(\left(K_{Z_o}{}^2 - K_{X_o}{}^2\right)\cos\eta\sin\eta\right)$

C_L lift coefficient (Lift/qS)

C_n yawing-moment coefficient (Yawing moment/qSb)

C_l rolling-moment coefficient (Rolling moment/qSb)

C_Y lateral-force coefficient (Lateral force/qS)

C_{Y_β} rate of change of lateral-force coefficient with angle of sideslip, per degree or per radian, as specified $(\partial C_Y/\partial\beta)$

C_{n_β} rate of change of yawing-moment coefficient with angle of sideslip, per degree or per radian, as specified $(\partial C_n/\partial\beta)$

C_{l_β} rate of change of rolling-moment coefficient with angle of sideslip, per degree or per radian, as specified $(\partial C_l/\partial\beta)$

C_{Y_p} rate of change of lateral-force coefficient with rolling-angular-velocity factor, per radian $\left(\frac{\partial C_Y}{\partial\frac{pb}{2V}}\right)$

C_{l_p} rate of change of rolling-moment coefficient with rolling-angular-velocity factor, per radian $\left(\frac{\partial C_l}{\partial\frac{pb}{2V}}\right)$

C_{n_p} rate of change of yawing-moment coefficient with rolling-angular-velocity factor, per radian $\left(\frac{\partial C_n}{\partial \frac{pb}{2V}}\right)$

C_{l_r} rate of change of rolling-moment coefficient with yawing-angular-velocity factor, per radian $\left(\frac{\partial C_l}{\partial \frac{rb}{2V}}\right)$

C_{n_r} rate of change of yawing-moment coefficient with yawing-angular-velocity factor, per radian $\left(\frac{\partial C_n}{\partial \frac{rb}{2V}}\right)$

C_{Y_r} rate of change of lateral-force coefficient with yawing-angular-velocity factor, per radian $\left(\frac{\partial C_Y}{\partial \frac{rb}{2V}}\right)$

l tail length (distance from center of gravity to rudder hinge line), feet

$\bar{z}$ height of center of pressure of vertical tail above fuselage axis, feet

p rolling-angular velocity, radians per second

r yawing-angular velocity, radians per second

D_b differential operator (d/ds_b)

s_b distance along flight path, spans (Vt/b)

λ complex root of stability equation $(c \pm id)$

t time, seconds

P period of oscillation, seconds

$T_{1/2}$ time for amplitude of oscillation to change by factor of 2 (positive value indicates a decrease to half-amplitude, negative value indicates an increase to double amplitude)

EQUATIONS OF MOTION

The nondimensional lateral equations of motion (reference 2), referred to a stability-axes system (fig. 2), are:

In roll –

$$2\mu_b\left(K_X^2 D_b^2\phi + K_{XZ} D_b^2\psi\right) = C_{l_\beta}\beta + \frac{1}{2} C_{l_p} D_b\phi + \frac{1}{2} C_{l_r} D_b\psi$$

In yaw –

$$2\mu_b\left(K_Z^2 D_b^2\psi + K_{XZ} D_b^2\phi\right) = C_{n_\beta}\beta + \frac{1}{2} C_{n_p} D_b\phi + \frac{1}{2} C_{n_r} D_b\psi$$

In sideslip –

$$2\mu_b(D_b\beta + D_b\psi) = C_{Y_\beta}\beta + \frac{1}{2} C_{Y_p} D_b\phi + C_L\phi + \frac{1}{2} C_{Y_r} D_b\psi + (C_L \tan\gamma)\psi$$

When $\phi_o e^{\lambda s_b}$ is substituted for ϕ, $\psi_o e^{\lambda s_b}$ for ψ, and $\beta_o e^{\lambda s_b}$ for β in the equations written in determinant form, λ must be a root of the stability equation

$$A\lambda^4 + B\lambda^3 + C\lambda^2 + D\lambda + E = 0 \qquad (1)$$

where

$$A = 8\mu_b^3\left(K_X^2 K_Z^2 - K_{XZ}^2\right)$$

$$B = -2\mu_b^2\left(2K_X^2 K_Z^2 C_{Y_\beta} + K_X^2 C_{n_r} + K_Z^2 C_{l_p} - 2K_{XZ}^2 C_{Y_\beta} - K_{XZ} C_{l_r} - K_{XZ} C_{n_p}\right)$$

$$C = \mu_b\left(K_X^2 C_{n_r} C_{Y_\beta} + 4\mu_b K_X^2 C_{n_\beta} + K_Z^2 C_{l_p} C_{Y_\beta} + \frac{1}{2} C_{n_r} C_{l_p} - K_{XZ} C_{l_r} C_{Y_\beta}\right.$$

$$- 4\mu_b K_{XZ} C_{l_\beta} - C_{n_p} K_{XZ} C_{Y_\beta} - \frac{1}{2} C_{n_p} C_{l_r} + K_{XZ} C_{n_\beta} C_{Y_p} - K_Z^2 C_{Y_p} C_{l_\beta}$$

$$\left. - K_X^2 C_{Y_r} C_{n_\beta} + K_{XZ} C_{Y_r} C_{l_\beta}\right)$$

$$D = -\frac{1}{4} C_{n_r} C_{l_p} C_{Y_\beta} - \mu_b C_{l_p} C_{n_\beta} + \frac{1}{4} C_{n_p} C_{l_r} C_{Y_\beta} + \mu_b C_{n_p} C_{l_\beta} + 2\mu_b C_L K_{XZ} C_{n_\beta}$$

$$- 2\mu_b C_L K_Z^2 C_{l_\beta} - 2\mu_b K_X^2 C_{n_\beta} C_L \tan\gamma + 2\mu_b K_{XZ} C_{l_\beta} C_L \tan\gamma$$

$$+ \frac{1}{4} C_{l_p} C_{n_\beta} C_{Y_r} - \frac{1}{4} C_{n_p} C_{l_\beta} C_{Y_r} - \frac{1}{4} C_{l_r} C_{n_\beta} C_{Y_p} + \frac{1}{4} C_{n_r} C_{l_\beta} C_{Y_p}$$

$$E = \frac{1}{2} C_L \left(C_{n_r} C_{l_\beta} - C_{l_r} C_{n_\beta} \right) + \frac{1}{2} C_L \tan\gamma \left(C_{l_p} C_{n_\beta} - C_{n_p} C_{l_\beta} \right)$$

The damping and period of the lateral oscillation in seconds are given respectively by the equations $T_{1/2} = -\frac{0.69}{c}\frac{b}{V}$ and $P = \frac{2\pi}{d}\frac{b}{V}$ where c and d are the real and imaginary parts of the complex root of the stability equation.

The necessary and sufficient conditions for neutral oscillatory stability as shown in reference 3 are that the coefficients of the stability equation satisfy Routh's discriminant set equal to zero

$$R = BCD - AD^2 - B^2E = 0$$

and that the coefficients B and D have the same sign. In general, the sign of the B coefficient is determined by the factors $-C_{Y_\beta}$, $-C_{n_r}$, and $-C_{l_p}$ which appear in the predominant terms of B. Thus, B is positive in the usual case in which there is positive weathercock stability and positive damping in roll. Hence the coefficient D must be positive if R = 0 is a neutral-oscillatory-stability boundary.

CALCULATIONS

Calculations were made of the neutral-oscillatory-stability boundary for the two different loading conditions representing the airplane with wing-tip fuel tanks and the airplane without wing-tip fuel tanks. These two loading conditions simulate a change in the fuel load from a belly fuel tank to wing-tip tanks and, in effect, vary the radii of gyration in roll and yaw while the airplane weight is maintained approximately the same.

The roots of the stability equation were also computed for several combinations of C_{n_β}, C_{l_β}, and C_{n_p} to determine the period and time

to damp to one-half amplitude of the oscillatory and aperiodic modes of motion.

The aerodynamic and mass characteristics assumed for use in the calculations are presented in table I. Values of $C_{n_{\beta(\text{tail off})}}$ and $C_{Y_{\beta(\text{tail off})}}$ were estimated from force tests made on the Langley free-flight-tunnel six-component balance (reference 4) on a model representing the type of airplane assumed in the calculations. The tail-off values of C_{n_r}, C_{l_r}, C_{Y_r}, C_{l_p}, and C_{Y_p} were estimated from data taken in the Langley stability tunnel. The contributions of the tail to the stability derivatives were estimated from the equations given in the footnote of table I and are similar to those given in reference 5.

RESULTS AND DISCUSSION

Airplane with Wing-Tip Tanks

The results of the calculations to determine the effect of varying C_{n_p} on the neutral-oscillatory-stability boundary of the model with wing tip tanks are presented in figure 3 in the form of a stability chart in which the neutral-oscillatory-stability boundaries are plotted as a function of the directional-stability derivative C_{n_β} and the effective-dihedral derivative C_{l_β}.

The results indicate that, for values of C_{n_p} of 0.25, 0.30, and 0.40, branches of the neutral-oscillatory-stability boundary exist for both negative and positive values of C_{l_β}, whereas for values of C_{n_p} of −0.05, −0.1, 0.05, and 0.15 the neutral-oscillatory-stability boundary only appears for negative values of C_{l_β}; that is, in the first quadrant. An $R = 0$ curve for C_{n_p} of −0.05, −0.1, 0.05 and 0.15 does appear in the second quadrant but it is not a neutral-oscillatory-stability boundary because the D coefficient for these values of C_{n_p} is negative. Also, the dashed portions of the $R = 0$ curve for C_{n_p} of 0.25, 0.30, and 0.40 in the first quadrant are not neutral-oscillatory-stability boundaries because the D coefficient is negative. The relation between the D and R boundaries for $C_{n_p} = 0.4$ is illustrated in figure 4. The coefficient D is negative in the region below the $D = 0$ boundary. For the case where the $R = 0$ boundary is below the $D = 0$ boundary, there exists a negative D coefficient and hence the dashed portion

of the $R = 0$ curve is not a neutral-oscillatory-stability boundary. Although figure 4 is presented only for the case of $C_{n_p} = 0.40$, the conclusions drawn from this figure are also applicable to the other cases.

Where two branches of the neutral-oscillatory-stability boundary do exist, the significance of the boundaries can be determined by investigating the period of the neutrally stable oscillation for points located on each of the branches. As shown in reference 3, the period is proportional to $\sqrt{\frac{B}{D}}$; therefore, the branch of the neutral-oscillatory-stability boundary which is located near the $D = 0$ boundary, where the value of D is small for combinations of C_{n_β} and C_{l_β} located on this branch, represents the neutral-oscillatory-stability boundary of a long-period oscillation.

The part of the curves shown as solid lines for values of C_{n_p} of 0.25, 0.30 and 0.40 in the first quadrant (fig. 3) represent neutral-oscillatory-stability boundaries of a long-period oscillation. The other branches of the curves for C_{n_p} equal to 0.25, 0.30, and 0.40 in the second quadrant, and the curves of C_{n_p} equal to -0.05, -0.10, 0.05, and 0.15 represent neutral-oscillatory-stability boundaries of the normal short-period oscillation. The results of figure 3 indicate that as C_{n_p} varies from a negative to a small positive value, a stabilizing shift in the oscillatory-stability boundary occurs. Further increases in the positive value of C_{n_p}, however, result in a large destabilizing shift of the neutral-oscillatory-stability boundary.

A better indication of the meaning of the boundaries can be seen from a study of the damping and period of the oscillation and the damping of the aperiodic mode obtained from the roots of the lateral stability equation. The reciprocal of the time to damp to one-half amplitude has been used herein to express damping because it was desired to express the degree of stability as a direct rather than as an inverse function of the ordinate. Peak positive ordinates consequently indicate maximum damping and negative ordinates indicate negative (unstable) damping. The results presented in table II were obtained from roots calculated for the case of $C_{n_p} = 0.40$ at $C_{n_\beta} = 0.00227$ per degree and $C_{n_\beta} = 0.00100$ per degree while C_{l_β} was varied. The conditions listed in table II are identified by circled numbers in figure 3. Table II shows that when the neutral-oscillatory-stability boundary is crossed $\left(\text{from } C_{l_\beta} = 0.0025 \text{ per deg to } C_{l_\beta} = 0.0010 \text{ per deg}\right)$, the short-period oscillation becomes stable. This oscillation continues to remain stable as the

value of C_{l_β} is increased negatively. However, at $C_{l_\beta} = -0.0032$ per degree, a long-period oscillation appears and as the neutral-oscillatory-stability boundary is crossed (from $C_{l_\beta} = -0.0049$ per deg to $C_{l_\beta} = -0.00550$ per deg), the long-period oscillation becomes unstable. Table II also shows that the $R = 0$ curve in the second quadrant $\left(C_{n_\beta} = 0.00100\right)$ is a neutral-oscillatory-stability boundary for the short-period oscillation but that the dashed portion of $R = 0$ curve in the first quadrant is not a neutral-oscillatory-stability boundary.

Results of calculations made to show the effect of varying C_{n_p} on the period and damping characteristics of the oscillatory and aperiodic modes are shown in figure 5. These calculations were made for a given value of C_{n_β} and C_{l_β} (point Ⓐ in fig. 3) and show that increasing C_{n_p} in a positive direction causes an increase in the damping of the short-period oscillation throughout the C_{n_p} range investigated.

Airplane without Wing-Tip Tanks

The effect of C_{n_p} on the neutral-oscillatory-stability boundary for the model without wing-tip tanks is shown in figure 6. The $R = 0$ curves for C_{n_p} values of −0.05 and −0.10 are neutral-oscillatory-stability boundaries for the short-period oscillation. The solid portions of the $R = 0$ curves in the first quadrant for C_{n_p} of 0.10, 0.20, and 0.40 are neutral-oscillatory-stability boundaries of the long-period oscillation, whereas the corresponding branches of the boundaries in the second quadrant are neutral-oscillatory-stability boundaries for the short-period oscillation. The damping and period data were calculated from the roots of the stability equation by varying C_{n_p} for a given value of C_{n_β} and C_{l_β} (point Ⓑ in fig. 6). The results of these calculations are presented in figure 7 and indicate that the damping of the short-period oscillation increased as C_{n_p} was increased in a positive direction.

A comparison of figures 5 and 7 indicates that shifting fuel from the fuselage to wing-tip tanks caused a decrease in the damping of the short-period oscillation for all values of C_{n_p} investigated. (The data of figures 5 and 7 were computed for different combinations of C_{n_β} and C_{l_β} but it is assumed that at least a qualitative comparison can be made of these results.)

For extreme positive values of C_{n_p} in both loading conditions the damping of the aperiodic modes, which are normally highly damped, was reduced to nearly zero.

CONCLUSIONS

From the results of the investigation made to determine the effect on the oscillatory stability of varying C_{n_p} (rate of change of yawing-moment coefficient with the rolling-angular-velocity factor) the following conclusions are drawn:

1. Increasing C_{n_p} in a positive direction increased the damping of the short-period oscillation for all values of C_{n_p}.

2. For any given value of C_{n_p} shifting fuel from the fuselage to external wing-tip tanks decreased the damping of the short-period oscillation.

Langley Aeronautical Laboratory
National Advisory Committee for Aeronautics
Langley Field, Va., July 23, 1948

REFERENCES

1. Toll, Thomas A., and Queijo, M. J.: Approximate Relations and Charts for Low-Speed Stability Derivatives of Swept Wings. NACA TN No. 1581, 1948.

2. Sternfield, Leonard: Some Considerations of the Lateral Stability of High-Speed Aircraft. NACA TN No. 1282, 1947.

3. Routh, Edward John: Dynamics of a System of Rigid Bodies. Pt. II. Macmillan and Co., Ltd., 1930.

4. Shortal, Joseph A., and Draper, John W.: Free-Flight-Tunnel Investigation of the Effect of the Fuselage Length and the Aspect Ratio and Size of the Vertical Tail on Lateral Stability and Control. NACA ARR No. 3D17, 1943.

5. Bamber, Millard J.: Effect of Some Present-Day Airplane Design Trends on Requirements for Lateral Stability. NACA TN No. 814, 1941.

TABLE I

CHARACTERISTICS OF AIRPLANE USED IN THE CALCULATIONS

Items	Without wing-tip tanks	With wing-tip tanks
W, lb	16,500	15,700
W/S	47.3	44.9
b, ft	39.7	39.7
ρ	0.00238	0.00238
μ_b	15.56	14.7
K_X	0.117	0.302
K_Z	0.226	0.405
l/b	0.643	0.643
$\bar{z}/b$	0.162	0.162
C_L	0.70	0.70
α, deg	12.0	12.0
ϵ, deg	5	5
η, deg	7	7
γ, deg	−10	−10
C_{Y_p}, per radian	0.40	0.40
C_{Y_r}, per radian	0	0
C_{Y_β}, per radian	$-0.115 + C_{Y_{\beta(tail)}}$	$-0.115 + C_{Y_{\beta(tail)}}$
[a] C_{n_β}, per radian	$-0.012 + C_{n_{\beta(tail)}}$	$-0.012 + C_{n_{\beta(tail)}}$
[a] C_{l_p}, per radian	$-0.30 + C_{l_{p(tail)}}$	$-0.35 + C_{l_{p(tail)}}$
[a] C_{n_p}, per radian	[b]Variable $+ C_{n_{p(tail)}}$	[b]Variable $+ C_{n_{p(tail)}}$
[a] C_{l_r}, per radian	$0.175 + C_{l_{r(tail)}}$	$0.175 + C_{l_{r(tail)}}$
[a] C_{n_r}, per radian	$-0.006 + C_{n_{r(tail)}}$	$-0.006 + C_{n_{r(tail)}}$
$C_{Y_{\beta(tail)}}$, per radian	[c]Variable	[c]Variable

[a]Tail contributions are determined from the following equations:

$$C_{n_{\beta(tail)}} = -\frac{l}{b} C_{Y_{\beta(tail)}}$$

$$C_{l_{p(tail)}} = 2\left(\frac{\bar{z}}{b} - \frac{l}{b}\sin\alpha\right)^2 C_{Y_{\beta(tail)}}$$

$$C_{n_{p(tail)}} = C_{l_{r(tail)}} = -2\,\frac{l}{b}\left(\frac{\bar{z}}{b} - \frac{l}{b}\sin\alpha\right) C_{Y_{\beta(tail)}}$$

$$C_{n_{r(tail)}} = 2\left(\frac{l}{b}\right)^2 C_{Y_{\beta(tail)}}$$

[b]Varied systematically as independent variable to provide the desired range of C_{n_p} for the determination of the stability boundaries.

[c]Varied systematically as independent variable to determine the effect of C_{n_β} on the stability boundaries.

TABLE II

PERIOD AND RECIPROCAL OF TIME FOR AIRPLANE WITH WING-TIP TANKS TO DAMP TO ONE-HALF AMPLITUDE

$[C_L = 0.70]$

Condition	C_{l_β} (per deg)	Oscillatory mode		Aperiodic mode
		P (sec)	$\frac{1}{T_{1/2}}$ (1/sec)	$\frac{1}{T_{1/2}}$ (1/sec)
$C_{n_\beta} = 0.00227$				
1	0.0025	2.10	−0.085	−0.253 3.135
2	.0010	2.11	.183	−.216 2.563
3	−.0032	2.02 75.22	1.048 .315	---------- ----------
4	−.00447	1.96 17.90	1.273 .089	---------- ----------
5	−.0049	1.93 15.99	1.359 .003	---------- ----------
6	−.0055	1.90 14.82	1.451 −.089	---------- ----------
$C_{n_\beta} = 0.0010$				
7	0.0010	3.11	−0.146	−0.153 2.793
8	−.0015	3.19	.861	−.265 .900
9	−.0030	2.81	1.385	−.575 .167
10	−.0040	2.60	1.595	−.870 .045

NACA

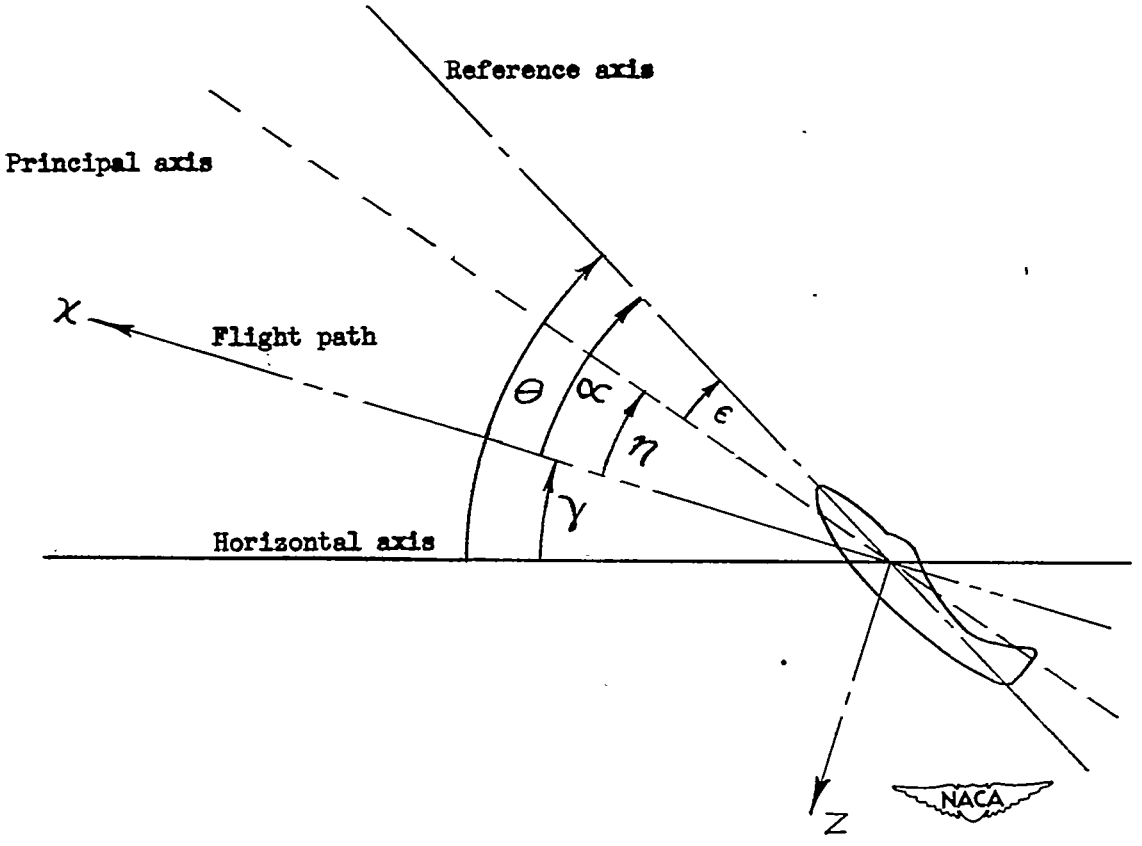

Figure 1.- System of axes and angular relationship in flight. Arrows indicate positive direction of angles. $\eta = \theta - \gamma - \epsilon$.

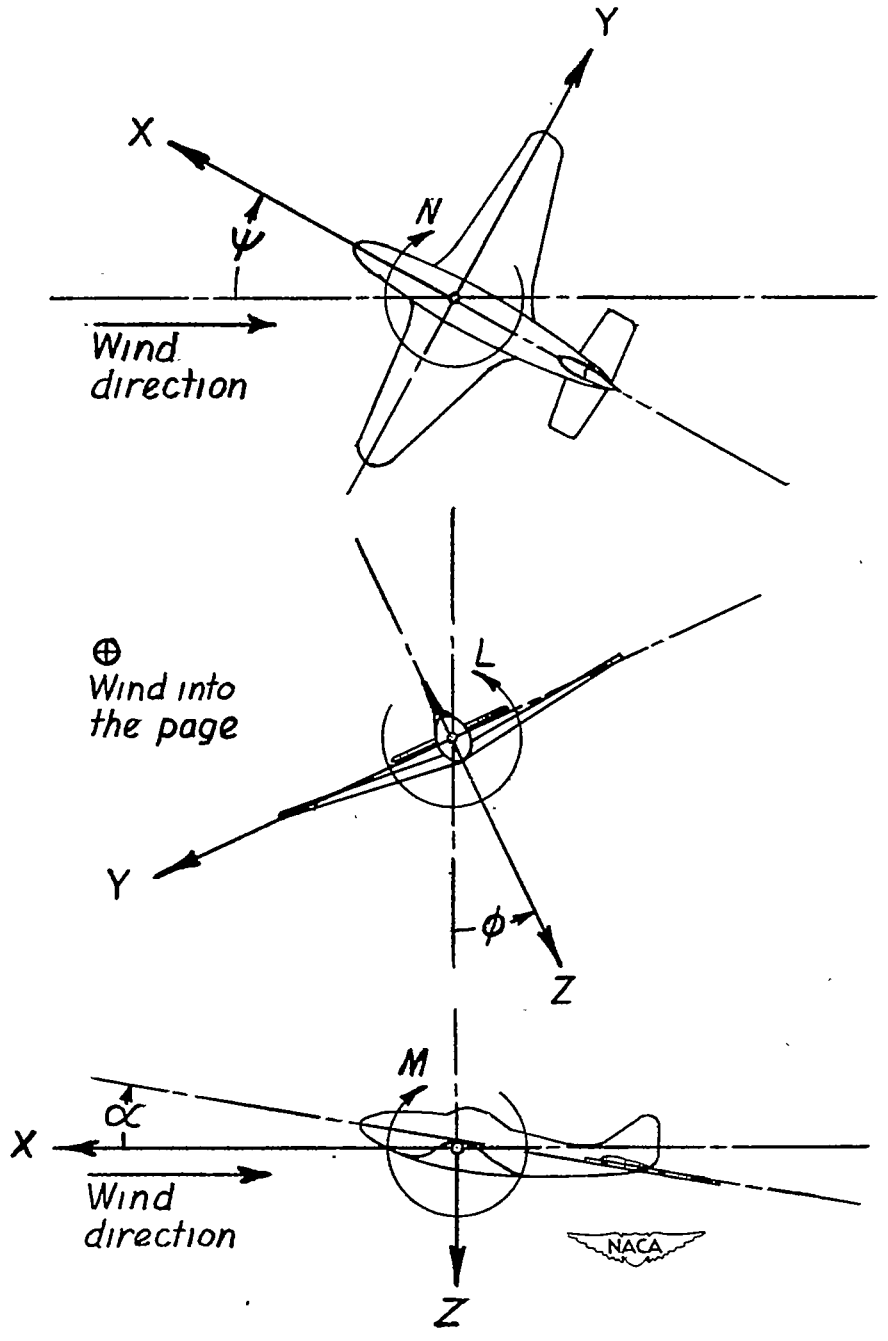

Figure 2.- The stability system of axes is defined as an orthogonal system of axes having their origin at the center of gravity and in which the Z-axis is in the plane of symmetry and perpendicular to the relative wind, the X-axis is in the plane of symmetry and perpendicular to the Z-axis, and the Y-axis is perpendicular to the plane of symmetry. Arrows indicate positive directions of moments and forces.

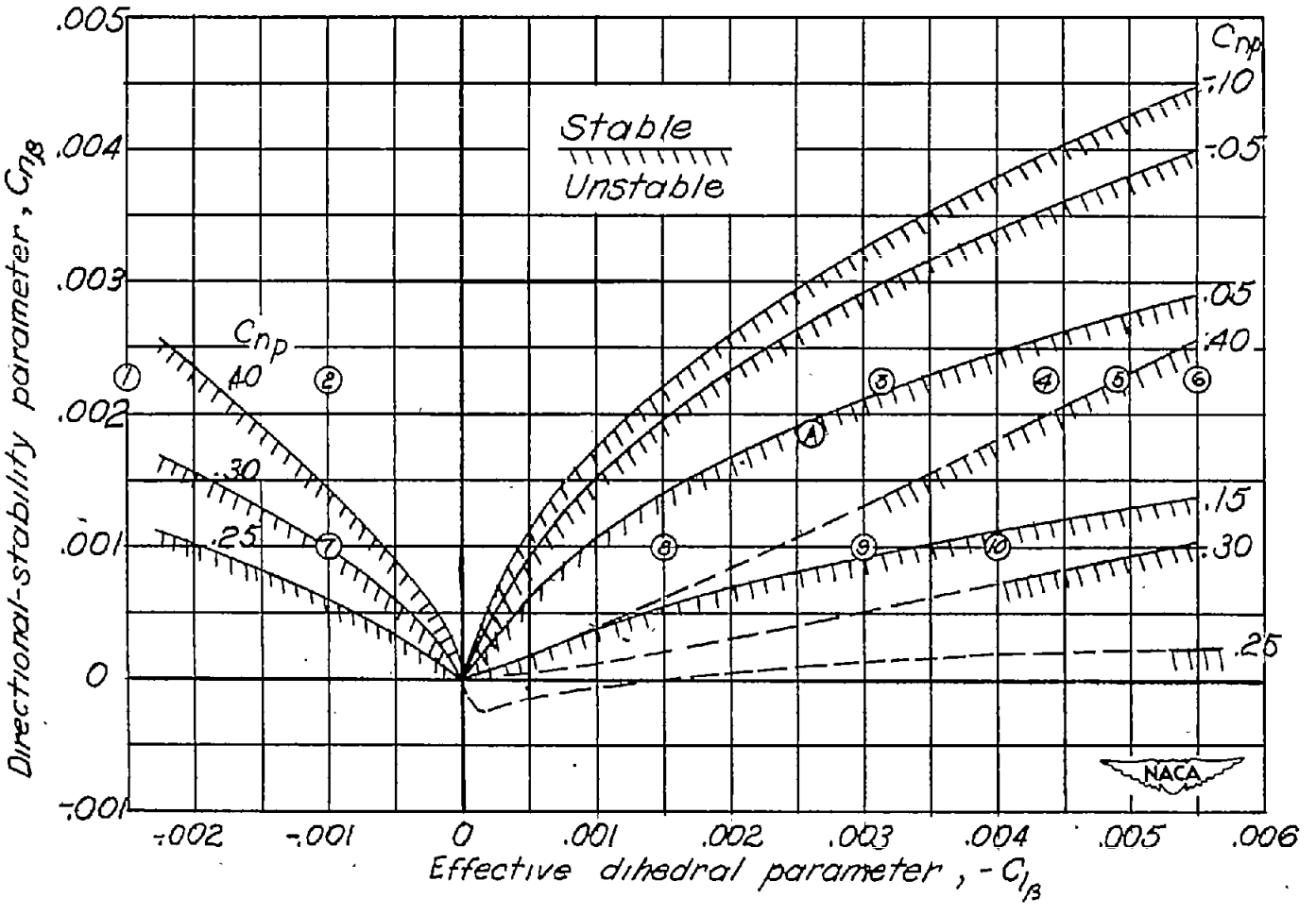

Figure 3.- Effect of the rotary derivative C_{n_p} on the neutral-lateral-oscillatory-stability boundary. $C_L = 0.70$. Airplane with wing-tip tanks. Circled numbers in figure are identified as conditions given in table II. The dashed-portion of the R = 0 boundary is not a neutral-lateral-oscillatory-stability boundary because the D coefficient of the lateral stability equation is negative.

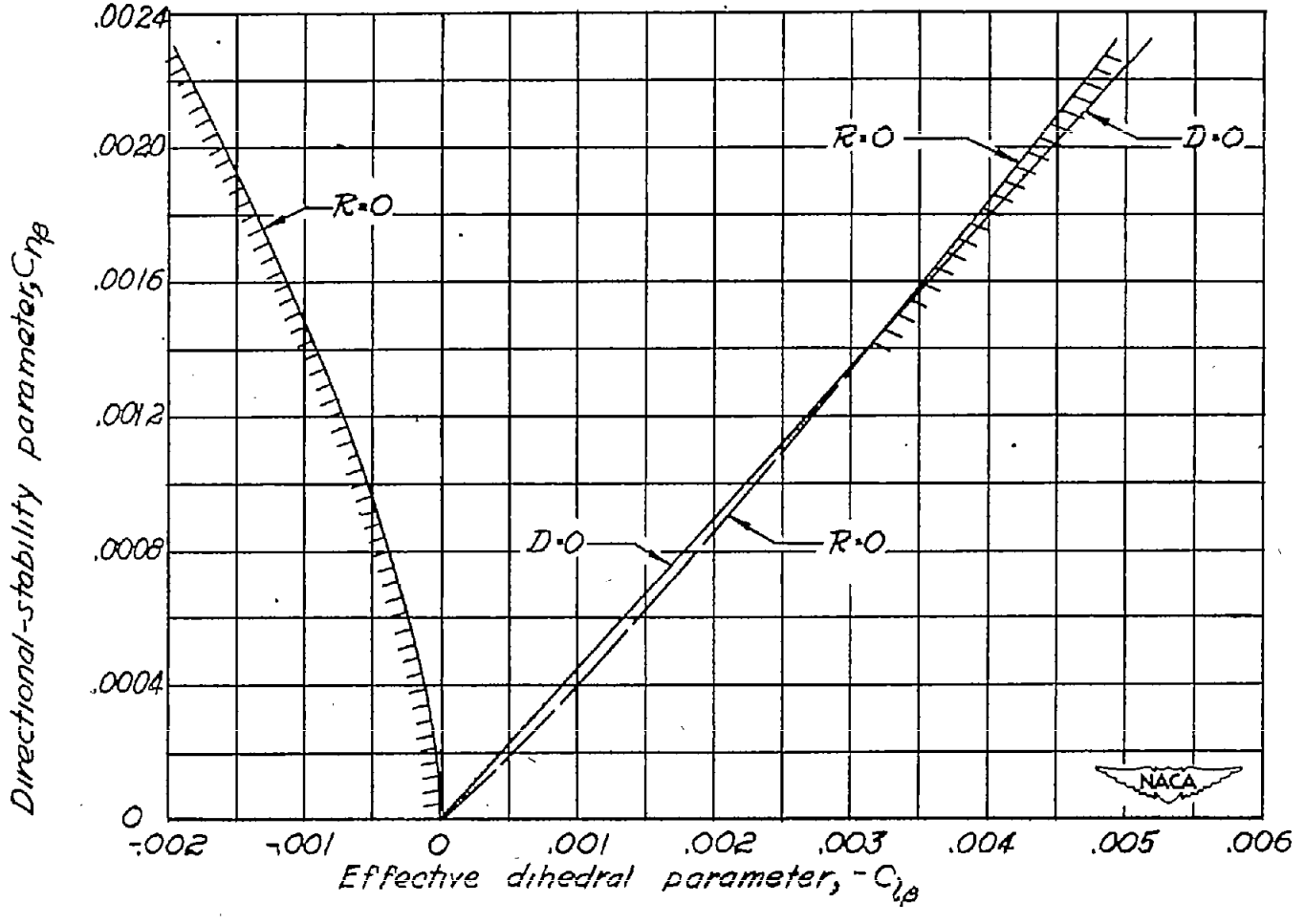

Figure 4.- Relative location of the D = 0 boundary with respect to the R = 0 boundary. The portion of the R = 0 boundary above the D = 0 boundary represents the neutral-lateral-oscillatory-stability boundary. $C_{n_p} = 0.40$; $C_L = 0.70$.

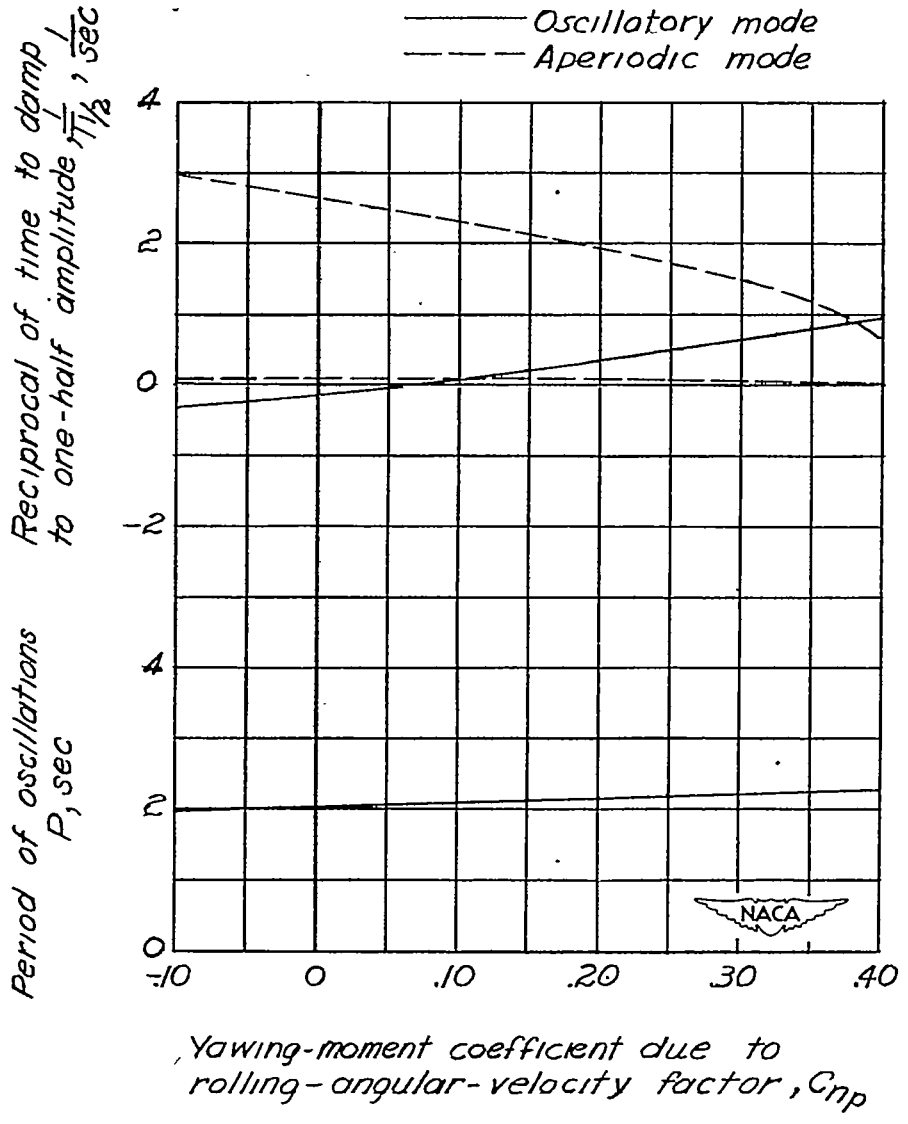

Figure 5.- Effect of the rotary derivative C_{n_p} on the damping and period of the oscillatory and aperiodic modes of a sweptback fighter-type airplane with wing-tip tanks. $C_{n_\beta} = 0.00186$ per degree; $C_{l_\beta} = -0.0026$ per degree; $C_L = 0.70$.

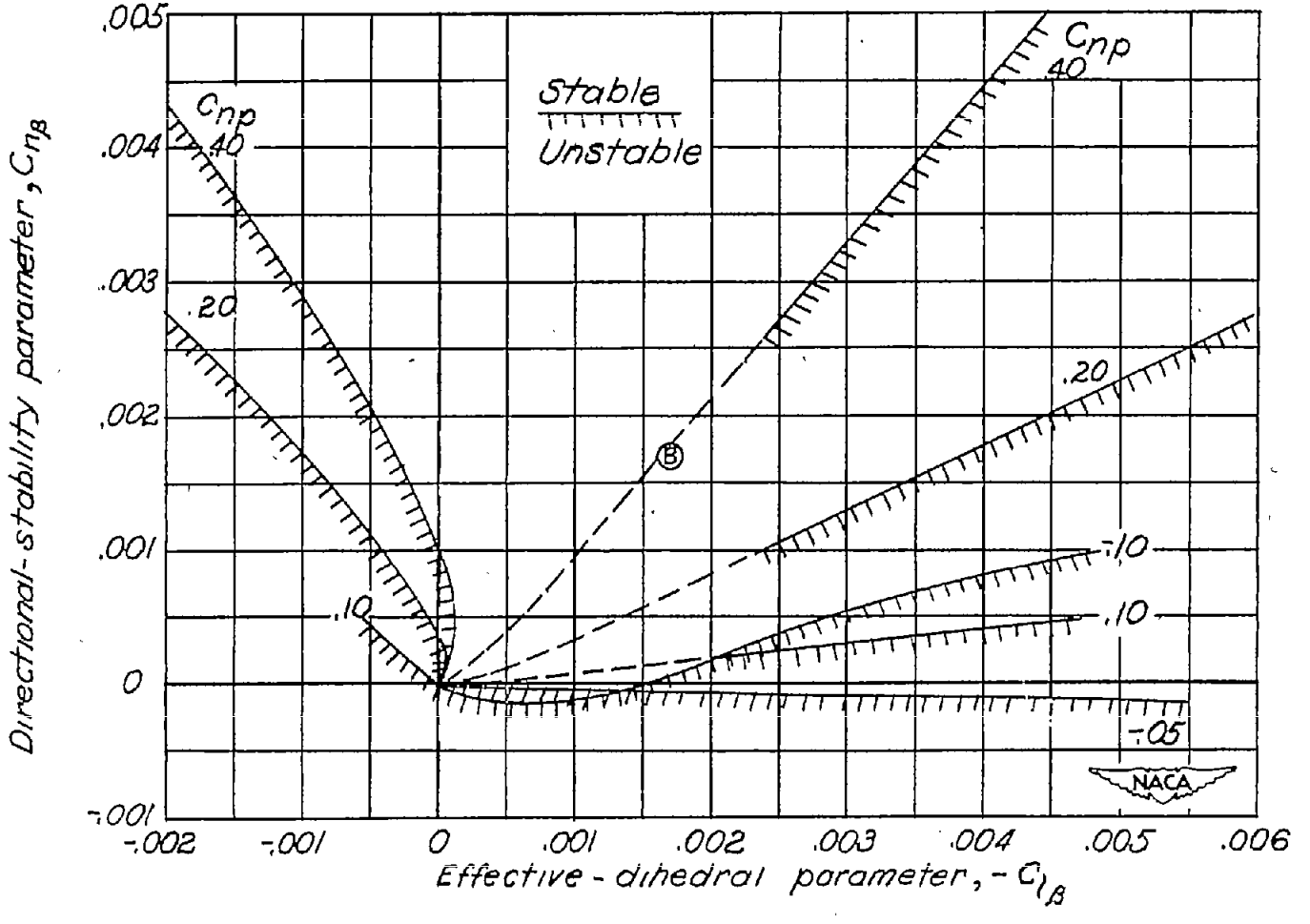

Figure 6.- Effect of the rotary derivative C_{n_p} on the neutral-lateral-oscillatory-stability boundary. Airplane without wing-tip tanks. C_L = 0.70. The dashed portion of the R = 0 boundary is not a neutral-lateral-oscillatory-stability boundary because the D coefficient of the lateral stability equation is negative.

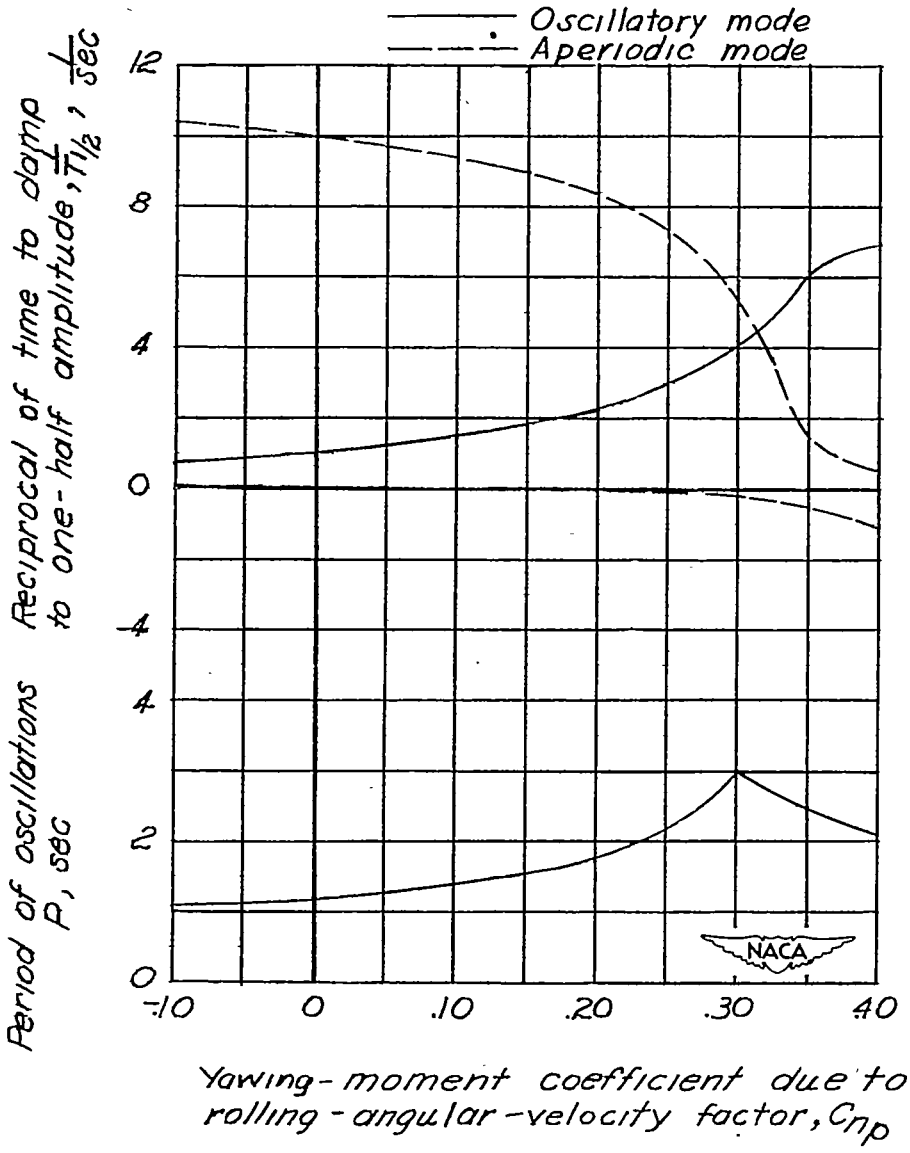

Figure 7.- Effect of the rotary derivative C_{n_p} on the damping and period of the oscillatory and aperiodic modes of a sweptback fighter-type airplane without wing-tip tanks. C_{n_β} = 0.0017 per degree; C_{l_β} = -0.0017 per degree; C_L = 0.70.